Journal of Power Sources 512 (2021) 230516

Contents lists available at ScienceDirect

Journal of Power Sources

journal homepage: www.elsevier.com/locate/jpowsour

Mitigating capacity fading in aqueous organic redox flow batteries through a simple electrochemical charge balancing protocol

Teresa Páez [a,b], Alberto Martínez-Cuezva [c], Rebeca Marcilla [a], Jesús Palma [a], Edgar Ventosa [a,d,e,*]

[a] IMDEA Energy, Avda. Ramón de La Sagra 3, E-28935, Móstoles, Madrid, Spain
[b] Departamento de Ingeniería Química Industrial y del Medio Ambiente, Escuela Técnica Superior de Ingenieros Industriales, Universidad Politécnica de Madrid, C/José Gutierrez Abascal, 2, 28006, Madrid, Spain
[c] Departamento de Química Orgánica, Facultad de Química, Regional Campus of International Excellence "Campus Mare Nostrum", Universidad de Murcia, E-30100, Murcia, Spain
[d] Departamento de Química, Universidad de Burgos, Pza. Misael Bañuelos S/n, E-09001, Burgos, Spain
[e] International Research Centre in Critical Raw Materials-ICCRAM, University of Burgos, Plaza Misael Bañuelos S/n, E-09001, Burgos, Spain

HIGHLIGHTS

- Charge imbalance is identified as a significant cause for capacity fading
- Implementation of the charging protocol reverses capacity losses
- Capacity retention is remarkable enhanced by this charging protocol
- This protocol is a general approach for redox flow batteries
- Implementation of this protocol is simple and inexpensive

GRAPHICAL ABSTRACT

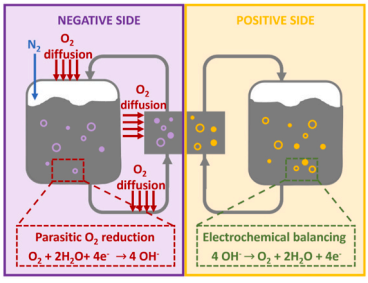

ABSTRACT

Aqueous organic redox flow batteries (AORFBs) have recently been attracting much attention due to their potential utilization as a sustainable solution for stationary energy storage. However, AORFBs have still to face various challenges to become a competitive technology to other mature redox flow batteries. Fading of the energy storage capacity upon cycling leading to insufficient lifetime is likely the most pressing issue. Several processes are contributing to this issue. Among the capacity fading promoters, the existence of side reactions such as water splitting and reactions related to oxygen reduction triggers an imbalanced state of charge for the catholyte and anolyte. Herein, a simple electrochemical balancing procedure is proposed and successfully demonstrated through the restoration of the oxidation states of the two half-cell solutions. The results reveal that it is possible to mitigate and even revert the effects of such side reactions, developing a useful method for mitigating the capacity fading and prolonging the cycling performance of AORFBs. In the two case studies, the implementation of this simple charging procedure leads to a remarkable 20-fold reduction of capacity fading (% h^{-1}). The protocol is a general approach for redox flow batteries, easily implementable and inexpensive.

1. Introduction

Electrochemical Energy Storage (EES) technologies have increasingly become important as an element to power electric vehicles or hand-held electronics, and they are considered critical in the development of sustainable electrical grid systems [1,2]. Redox flow batteries

* Corresponding author. IMDEA Energy, Avda. Ramón de La Sagra 3, E-28935, Móstoles, Madrid, Spain.
E-mail address: eventosa@ubu.es (E. Ventosa).

https://doi.org/10.1016/j.jpowsour.2021.230516
Received 11 March 2021; Received in revised form 29 July 2021; Accepted 7 September 2021
Available online 14 September 2021

(RFBs) are especially suitable for stationary energy storage applications since their unique architecture, with decoupled energy and power, allows them to be scaled more effectively than conventional batteries [3,4]. To date, the most developed and commercialized RFBs are based on metal ions, mostly vanadium, dissolved in strongly acidic solutions [5,6]. Despite their competitive electrochemical performance, large scale implementation of metal-based RFBs poses a sustainability challenge that impels researchers to look for new battery chemistries based on sustainable redox-active organic molecules built on non-critical elements, such as C, H, O, N or S. Thus, aqueous organic redox flow batteries (AORFBs), in which the inorganic species are replaced by organic-based compounds, appear to be a very promising approach [7]. Although various chemistries have shown to deliver competitive performances in terms of energy density, power density, energy efficiency and potential cost, cycle stability (a critical parameter for stationary applications) still raises concern [8].

The energy storage capacity of a battery evolves upon cycling. The progressive decay in energy storage capacity is usually referred to as capacity fading. In traditional redox flow batteries, such capacity fading may be triggered by various performance-limiting factors. There are 3 prime sources of capacity fading including i) active species degradation (incompatibility, molecular decomposition) [9,10], ii) shortcomings in the flow cell engineering (crossover, leakage, membrane degradation) [11–13], or iii) charge imbalance (hydrogen and oxygen evolution, species oxidation with air) [14–16]. Consequently, the identification of mechanisms of the processes that provoke the capacity fading is essential to differentiate the contribution of each source and develop strategies to minimize them. For AORFBs in asymmetric configuration (different species in catholyte and anolyte), which is vastly the most frequent option, the three processes lead to capacity fading. This is indeed the main drawback compared to the state-of-the-art redox flow battery (the all-vanadium flow battery) for which the last two processes are reversible and the first one (degradation) does not occur.

Most efforts are being devoted to increasing the stability of organic compounds and thus preventing degradation. However, simple electrochemical evaluation of the (electro-)chemical stability is not straightforward since capacity fading cannot be simply deconvoluted due to the other two factors. One of the few examples addressing this point made use of in-situ NMR analysis to study the degradation processes of organic redox species in a flow battery [17]. Crossover of active species through the membrane is addressed by various approaches, such as i) increasing the size of the organic compounds to avoid the crossover by steric impediment [18] or ii) using bifunctional redox electrolyte (e.g. organic compounds with two redox processes being used in both catholyte and anolyte) [19]. In contrast, charge (faradaic) imbalance between the state of charge (SoC) of catholyte and anolyte due to the occurrence of electrochemical side reactions has not yet been addressed for AORFBs despite this issue has been recognized as a major challenge in All-Vanadium Redox Flow Batteries (AVRFBs)[[20,21]]. In AVRFBs, recent studies show the effectiveness of electrochemical strategies, which on the other hand require monitoring the SoC of catholyte and anolyte as well as the implementation of a secondary electrochemical device [22,23]. In AORFBs, expensive Ar-filled gloveboxes have been used to completely exclude the occurrence of reactions related to oxygen reduction in long-term cycling measurements, being an excellent approach for academic proposes. However, this strategy is neither accessible for most research groups nor practical for larger-scale implementation.

In this report, we present a general approach to revert the detrimental effects of parasitic reactions in capacity retention and help deconvolute their contribution to the overall capacity fading. This approach consists of a simple electrochemical charge balancing protocol, which allows water splitting to take place in one compartment to compensate the charges consumed in the opposite compartment by the undesired reactions. We explore the effectiveness of the strategy in two organic compound//ferrocyanide alkaline flow systems, i.e. anthraquinone-derivative//ferrocyanide, and phenazine-derivative//ferrocyanide, demonstrating the benefits of the proposed approach in their long-term cycle stability. The method presented here constitutes a step forward for the development of AORFBs as an inexpensive and sustainable solution in large-scale electrochemical energy storage.

2. Results and discussion

2.1. Capacity imbalance of AORFBs by side reactions

Energy storage through electrochemical reactions of active species that take place in opposite half-cells of any battery can only occur simultaneously due to the flow of electrons (externally) and ions (internally) between the two electrodes. Unfortunately, side reactions irreversibly consume electrons under operating conditions leading to an uneven state of charge of catholyte and anolyte, referred to as electrolyte A and electrolyte B, respectively. As a result, at the end of the charging process, electrolyte A will be fully charged while electrolyte B, in which side reactions took place, will not reach the fully charged state. In this case, electrolyte B will limit the subsequent discharging process, reducing the charge storage capacity of the system. In the following cycle, electrolyte A will not be fully discharged at the beginning of the next discharged process, so that the maximum charge storage capacity of the system will be permanently reduced. This mismatch in the state of charge between the catholyte and anolyte, which reduces the charge storage capacity of a system, is referred to as faradaic imbalance. Two separately electrochemical phenomena primarily contribute to the faradaic imbalance; i) electrolysis of electrolyte and ii) reactions related to oxygen reduction.

i. Electrolysis at the negative and positive electrode. The obvious drawback in aqueous electrochemical energy storage systems, compared to non-aqueous ones, is the narrower thermodynamic stability window of the electrolyte (1.23 V), which is limited by the electrolysis of water. During the charging process, oxygen and hydrogen evolution reactions (OER and HER) can occur at the positive and negative electrodes, respectively, giving rise to losses in the coulombic efficiency. Fig. 1 illustrates the general mechanism of capacity imbalance by the OER (Fig. 1a) and the HER (Fig. 1b) during one charge/discharge cycle. In Fig. 1.a, the positive electrode suffering the OER will not be fully charged (e.g. 99%) as the OER consumes a portion of the applied current (e.g. 1%), while the negative electrode will be able to reach the full state of charge (100%). During the discharging process, the positive electrode will be the limiting side since it was not fully charged. As a result, the discharge capacity of the battery will be limited to 99% of its capacity. Most importantly, in the subsequent charge step, the negative electrode will not start from a fully discharged state (only 99% of the species in the negative electrode are in its discharge state), so that the battery would have lost 1% of its initial charge storage capacity. In Fig. 1.b, the negative electrode suffers an identical process, although the HER is the irreversible reaction consuming part of the charges in this case.

ii. Reactions related to oxygen reduction at the negative compartment. Under this category, we englobe two reactions in which oxygen is involved. On the one hand, the electrochemical oxygen reduction reaction (ORR) will also consume charges leading to charge storage capacity losses by faradaic imbalance. On the other hand, chemical oxidation of reduced species by reduction of oxygen present in the negative electrolyte, e.g. reduced viologen is oxidized to viologen by oxygen present in the solution [24]. The imbalance mechanism due to the reactions related to oxygen reduction is quite similar to that of the HER (Fig. 1b): irreversible consumption of charges in the negative electrode during the charging process, preventing the anolyte to reach the fully charged state. The discharge capacity will be limited by the state of charge achieved in the negative electrode, while full discharging will not be achieved in the positive compartment (reducing the capacity of the subsequent cycle).

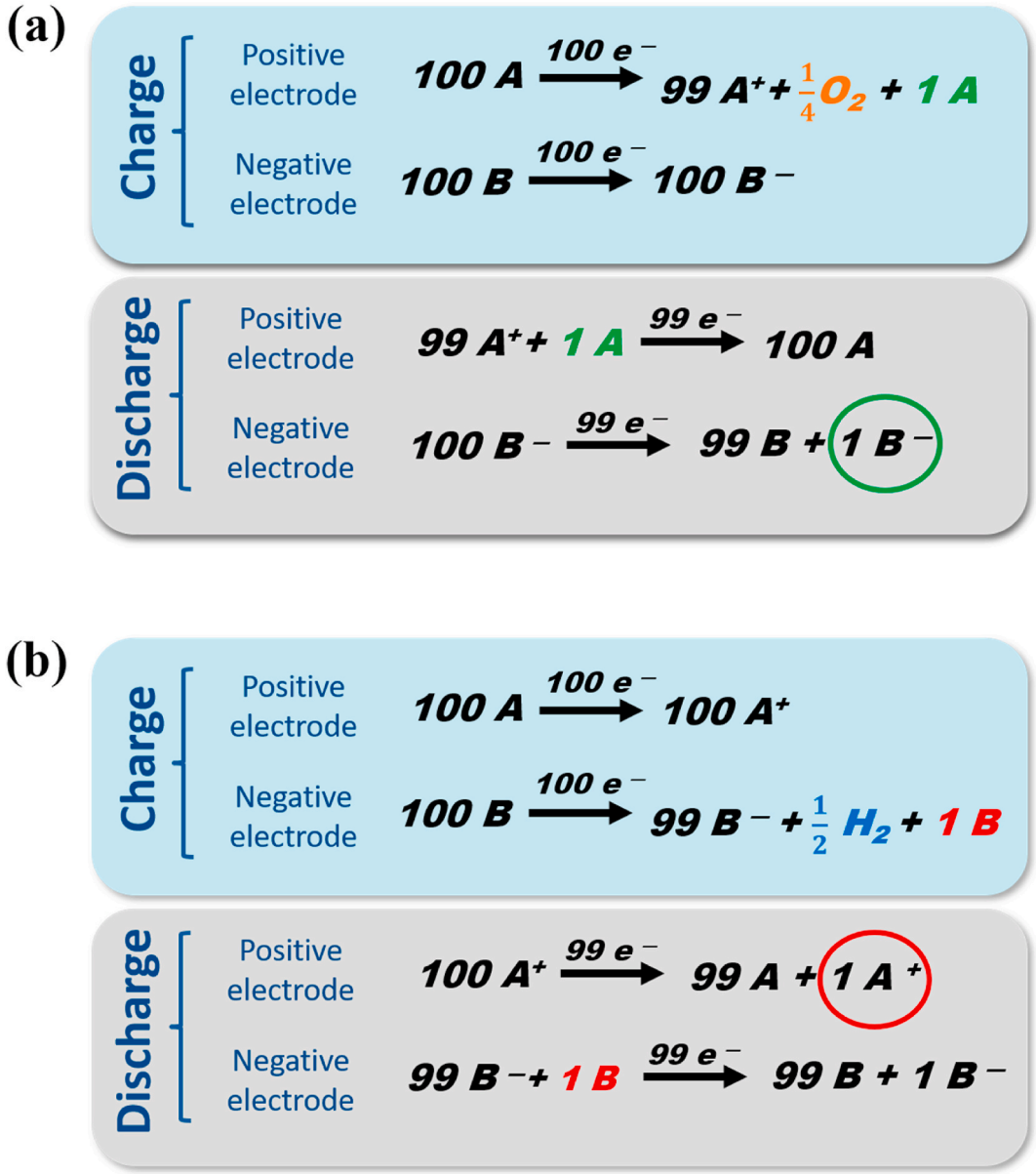

Fig. 1. Schematic illustration of the concept of battery imbalance in a flow battery during the first charge-discharge cycle, by (a) the OER in the positive electrode, (b) the HER in the negative electrode.

2.2. Electrochemical balancing protocol to revert capacity fading caused by faradaic imbalance

In practice, faradaic imbalance due to the reactions related to oxygen reduction is easily mitigated by displacing the oxygen dissolved in the electrolyte by an inert gas such as N_2 or Ar. The effect of faradaic imbalance due to the reactions related to oxygen reduction is clearly illustrated in Fig. 2 for the case of 2,6 dihydroxyanthraquinone (DHAQ)//ferrocyanide ($K_4Fe(CN)_6$) flow cells in alkaline media. Fig. 2.a shows the evolution of the charge storage capacity upon cycling in three different cases: open-air reservoirs, nitrogen-sealed reservoirs in 1 M KOH, and nitrogen-sealed reservoirs in 1.5 M KOH. When the anolyte contains large amounts of dissolved oxygen (open-air reservoirs), the faradaic imbalance due to the reactions related to oxygen reduction leads to a rapid capacity fading, losing the capacity to store energy after only 10 cycles. It should be noted that the solubility of O_2 at room temperature is about 0.25 mM. Considering that the ORR involves 4 electrons while anthraquinone 2 electrons, the ratio between the effective concentration of O_2 and anthraquinone is about 1:1000. Thus, charge imbalancing for an air-exposed system will depend on how fast oxygen dissolves in the anolyte and how long the charge/discharge cycles take. In our case, the entire cycle lasted 40-30 min and the charge imbalance was *ca.* 25 mAh (difference between two cycles). Thus, $6{\cdot}10^{-3}$ mmol of O_2 per min, which is reasonable considering the small liquid – gas contact area. In the case of nitrogen-sealed reservoirs, the system retained *ca.* 90% of their initial charge capacity after 50 cycles. In addition, the two measurements with nitrogen-sealed reservoirs (1.0 M KOH versus 1.5 M KOH) were carried out to evaluate the contribution of faradaic imbalance originated from water electrolysis since the concentration of KOH plays a role in the HER and the OER onset potentials. Fig. 2.a. shows that higher concentration of KOH results in a higher capacity retention (93% vs. 86%), which may be intuitively attributed to the hindrance of the HER. In general, the occurrence of undesired side reactions that lead to capacity fading decreases the coulombic efficiency of the charge/discharge cycle. Thus, the coulombic efficiency can be used to provide an estimation of the capacity fading due to faradaic

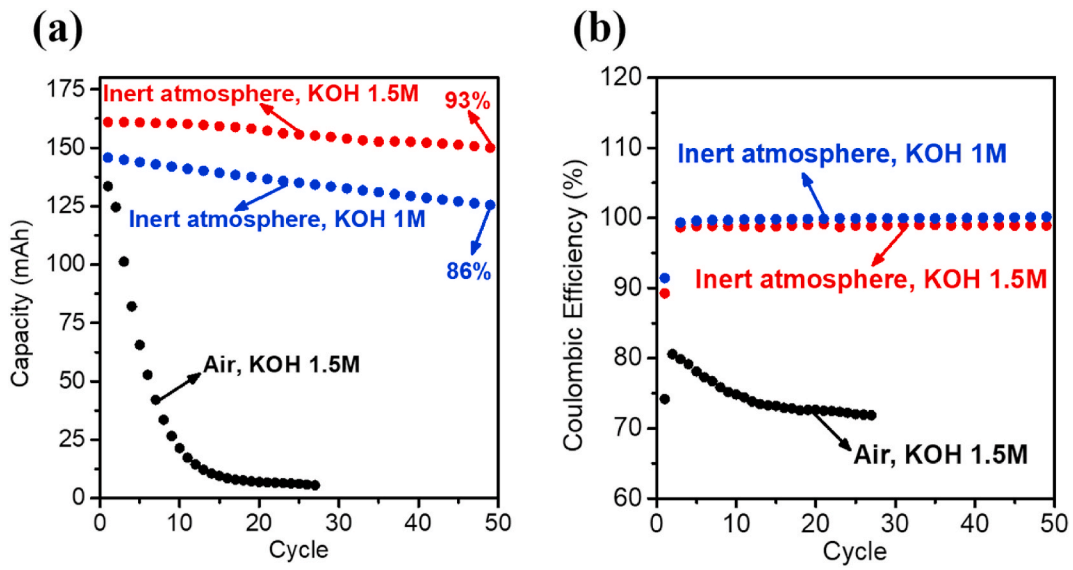

Fig. 2. Evidence of capacity fading by the REACTIONS RELATED TO OXYGEN REDUCTION in an anthraquinone//$K_4Fe(CN)_6$–flow cell in the absence and presence of inert atmosphere. Initially balanced cells with 20 mL of 0.3 M ferrocyanide in the positive reservoir and 20 mL of 0.3 M anthraquinone in the negative in 1.5 M KOH (red and black) or KOH 1 M eq (blue), were used for cycling at 20 mA·cm^{-2}. **(a)** Evaluation of charge capacity. **(b)** Coulombic efficiency versus number of cycles. (For interpretation of the references to colour in this figure legend, the reader is referred to the Web version of this article.)

imbalance, as shown in Fig. 2.b. As expected, the coulombic efficiency in an open-air reservoir configuration is significantly lower than those obtained in the N_2-sealed configuration. However, the coulombic efficiency in the cell using 1.5 M KOH is similar (even lower) than that in 1.0 M KOH, which does not support the trends observed in the capacity fading for those two cells. Thus, there is an unexpected side reaction that seems to be beneficial for the capacity retention, which begs the questions: what is it, and whether can we use it as a general strategy for rebalancing the charging in redox flow batteries?

A simplistic description of the faradaic imbalance is that charges consumed by an irreversible side reaction in one electrolyte are compensated by the accumulation of "charged species" in the opposite electrolyte. This means that one can intentionally promote the occurrence of an irreversible side reaction in the "imbalanced compartment", in which charged species are accumulated, to drive an accumulation of "charged species" at the opposite side. By doing this, the state of charge for both electrolytes will be "*rebalanced*" at the end of the charging process. For example, when reactions related to oxygen reduction in the anolyte are responsible for the faradaic imbalance, the promotion of the oxygen evolution reaction in the opposite electrolyte will compensate the charges irreversibly consumed by the reactions related to oxygen reduction. In the example of Fig. 2, the increase in the concentration of KOH also facilitates the OER at the positive electrode since redox potential for OER decreases with increasing pH, which could compensate for other irreversible reactions occurring at the negative electrode. The promotion of the OER by changing the concentration of KOH would lead to a more balanced state of charge of both electrolytes, while the coulombic efficiency would not necessarily increase.

Fig. 3a illustrates an AORFB in which oxygen unavoidably diffuses into the negative compartment. Note that diffusion of oxygen can only be prevented by placing the entire system inside a glovebox that continuously eliminates O_2 by continuous circulation of the atmosphere through a purification reactor. The oxygen reduction reaction (ORR) in the negative compartment not only leads to an imbalance state of charge of catholyte and anolyte, but it also varies slightly the pH. The reduction of oxygen will prevent the anolyte to reach full state of charge while the catholyte will. As a result, the anolyte will become the limiting side during the discharge, preventing the catholyte to reach fully discharged state. Upon cycling, the presence of oxygen in the negative compartment will lead to the accumulation of charge in the catholyte as illustrated in Fig. 3b. We propose to controllably promote the opposite reaction to the ORR in the other compartment, i.e. the Oxygen Evolution Reaction (OER) in the positive side as shown in Fig. 3a, by lifting the cut-off voltage to balance the state of charge of the electrolytes as well as the pH. Since that the ORR in the negative compartment leads to an accumulation of charged species in the positive compartment, the catholyte will reach full state of charge before the anolyte is fully charged. Thus, lifting the cut-off voltage will result in the occurrence of the OER in the positive side of the electrochemical reactor.

To further validate this hypothesis, a flow cell containing a balanced amount of anthraquinone and ferrocyanide was assembled for the evaluation of the effect of a special cycle (referred to as balancing cycle), in which the OER is intentionally promoted (Fig. 4). The evolution of the charge capacity is shown in Fig. 4.a. The cell was initially subjected to 10 cycles of a charge-discharge regime under an inert atmosphere of N_2 at 20 mAcm^{-2} and no significant capacity fading was observed. To promote reactions related to oxygen reduction and accelerate the capacity fading, the negative electrolyte was intentionally exposed to air from cycle 10. After only 12 cycles under air exposure, charge capacity dropped below 70% of its initial value, confirming the accelerated fading under favorable conditions for reactions related to oxygen reduction. The charges consumed by reactions related to oxygen reduction in the anolyte were compensated by the oxidation of the species in the catholyte, leading to the accumulation of "charged species" (ferricyanide) in the catholyte. As a consequence, the catholyte reaches the full state of charge before the anolyte is fully charged. Still, under air-exposed conditions, the upper cut-off voltage was shifted to higher values so that the OER was allowed to take place in the fully charged catholyte. By doing this, the anolyte was able to reach full charge balancing of the state of charge for both electrolytes. The discharge capacity in the balancing cycle increased with respect to the previous cycle since the occurrence of the OER in the catholyte during the charging process allowed both electrolytes to reach a higher state of charge at the end of the charging process. It should be noted that discharge capacity under air-exposed conditions and balancing protocol (cycles 25–30) is about 15 mAh lower than that obtained initially under N_2-atmosphere (cycles 1–10), which is attributed to the spontaneous reaction between reduced anthraquinone and dissolved oxygen during the discharge process. Fig. 4.b shows the voltage profile of the 2nd cycle under an inert atmosphere (before exposure to air when electrolytes

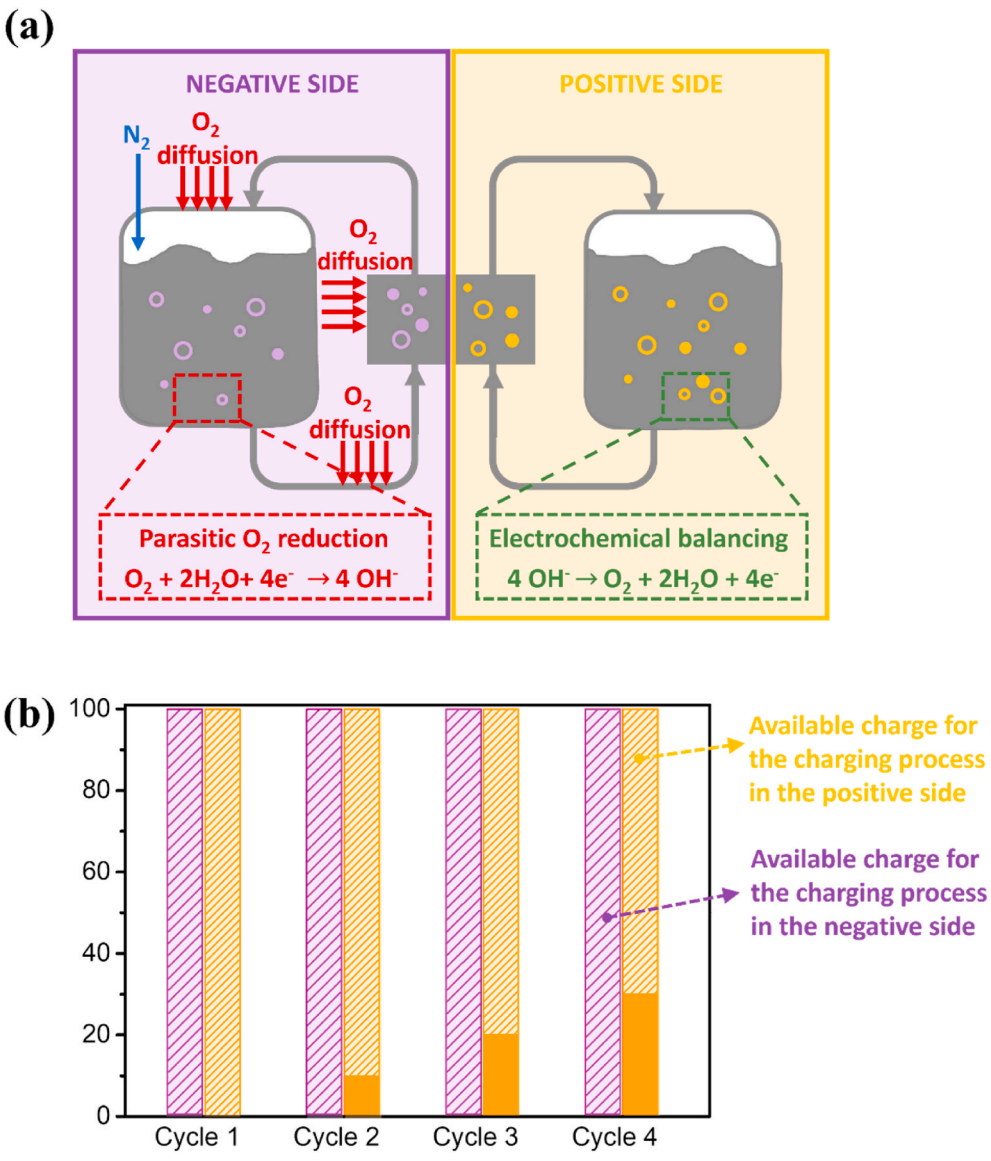

Fig. 3. **(a)** Illustration of a redox flow battery suffering of parasitic side reactions related to the presence of oxygen in the negative compartment. The opposite reaction (the oxygen evolution reaction) is proposed to be promoted controllably in the positive compartment to balance the state of charge of both positive and negative electrolytes. **(b)** Evolution of the state of charge of catholyte and anolyte at the fully discharged state (beginning of each cycle). The accumulation of "charged" species in the catholyte upon cycling due to the ORR in the negative compartment reduces the amount of species available for the charge process.

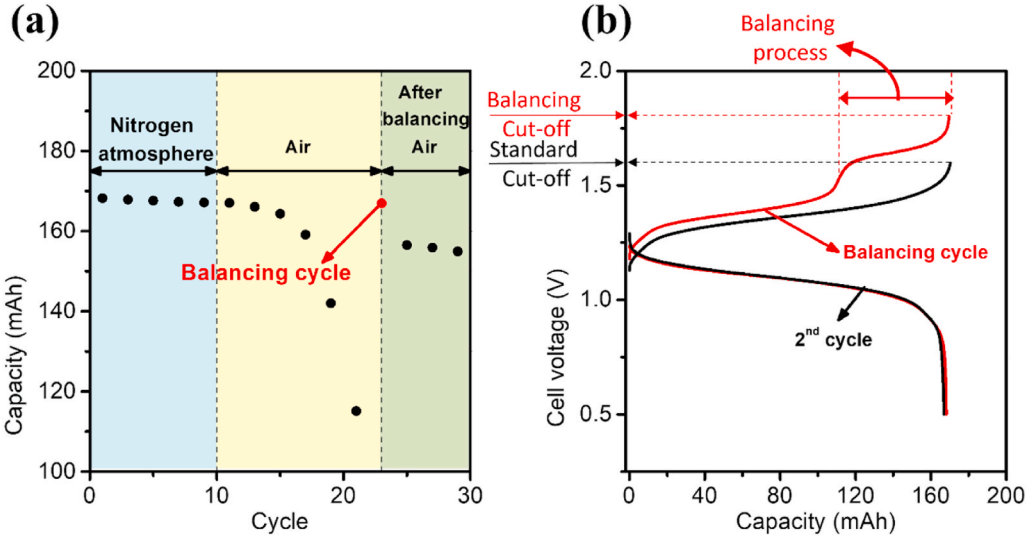

Fig. 4. Effect of the electrochemical balancing protocol in the charge storage capacity of alkaline DHAQ//$K_4Fe(CN)_6$ flow batteries (ferrocyanide 0.3 M as catholyte and anthraquinone 0.3 M as anolyte in KOH 1.5 M). The reservoirs were exposed to air after 10 cycles leading to a rapid capacity decay that was reverted by implementing the electrochemical balancing strategy. **(a)** Evolution of the charge storage capacity upon cycling. **(b)** Voltage profile of the 2nd cycle (before exposure to air when electrolytes were still balanced) and the electrochemical balancing cycle. Note that the upper cut-off voltage is increased from 1.6 V to 2.0 V for standard and balancing cycling protocols, respectively.

were still balanced) and the balancing cycle under air exposure. Note that the electrochemical balancing protocol consists in simply lifting the upper cut-off voltage during the charge process as illustrated in Fig. 4b. In the voltage profile during the charging process, a second plateau at higher voltage values appeared for the balancing cycle, which corresponds to the half-cell reactions of reduction of the anthraquinone and the OER at the negative and positive electrode, respectively. Most importantly, the discharge voltage profiles overlapped for the 2nd cycle and the balancing cycle, revealing that the faradaic imbalance attributed to reactions related to the presence of oxygen in the anolyte can be simply reversed by directly raising the upper cut-off voltage during one charging step allowing the OER to occur in the positive electrode. The assignment of the second plateau to the OER in the positive compartment instead of the HER in the negative side is based on two facts: I) The release of gas bubbles from the positive side of the electrochemical reactor during the second plateau as shown in the video in the Supplementary Information. II) Since the presence of oxygen prevents anthraquinone electrolyte to increase its state of charge adequately, the occurrence of a second irreversible side reaction in the same compartment would further hinder the anolyte to reach fully charged state, accelerating the capacity fading. Indeed, the imbalance between the state of charge of catholyte and anolyte would increase limiting even more the discharge capacity. Therefore, the occurrence of HER when the upper cut-off volatge is lifted would lead to increased capacity fading instead of the observed recovery of discharge capacity.

2.3. Long-term cycle stability test in alkaline flow batteries

The electrochemical balancing protocol is of high interest for the evaluation of long-term cycle stability of active compounds. Once the faradaic imbalance is compensated, the capacity fading can be attributed to the degradation and/or cross-over of active species.

Two state-of-the-art alkaline flow battery chemistries, namely of 2,6 dihydroxyanthraquinone//potassium ferrocyanide (DHAQ//$K_4Fe(CN)_6$) and 7,8-dihydroxyphenazine-2-sulfonic acid//potassium ferrocyanide (DHPS//$K_4Fe(CN)_6$), were used as study cases to further exemplify the impact of faradaic imbalance in the evaluation of long-term performances under N_2 atmosphere. Fig. 5 shows the electrochemical performance of two similar anthraquinone//ferrocyanide alkaline flow batteries that were cycled using two different operating protocols under a N_2 atmosphere. One flow battery (Fig. 5a) was charged and discharged using typical operation conditions (20 $mAcm^{-2}$ with a cut-off at 1.6V) and the second flow battery (Fig. 5b) was charged-discharged also at 20 $mAcm^{-2}$ but applying a balancing cycle (cut-off of 2V) every 10 cycles. The capacity fading observed using the traditional protocol was dramatically reduced by applying the balancing protocol (capacity fade decreased from 43% to ~2%). The difference in capacity fading is attributed to the presence of oxygen even when N_2 overpressure is applied to the negative reservoir. It should be noted that oxygen will diffuse by concentration gradient unless the atmosphere is regenerated (as occurred in a glovebox through the purification system). After these 100 cycles, the battery was operated at higher current densities (40 $mAcm^{-2}$) for 130 more cycles applying a balancing cycle with a cut-off of 2 V every 10 cycles (Fig. 4b). Finally, continuous balancing cycles (20 $mAcm^{-2}$ and cut-off of 2 V every cycle) were applied during the last 170 cycles (231–400) as shown in Fig. 5b. By implementing the electrochemical balancing protocol, the flow battery retained an impressive 90% of its initial storage capacity after 390 cycles (690 h) under N_2 atmosphere. Importantly, the implementation of the electrochemical balancing protocol clearly reduces the capacity fading from 0.24%·h^{-1} (0.43%·$cycle^{-1}$) to 0.0099% h^{-1} (0.018% $cycle^{-1}$) for the first 100 cycles. This value of capacity fading obtained using the electrochemical balancing protocol is close to the best value reported for this chemistry: 0.0058% h^{-1} when cycled at 88% depth of charge [25]. In that study, Aziz et al. reported that the source of this capacity fading was the dimerization process of the DHAQ, ruling out the occurrence of other

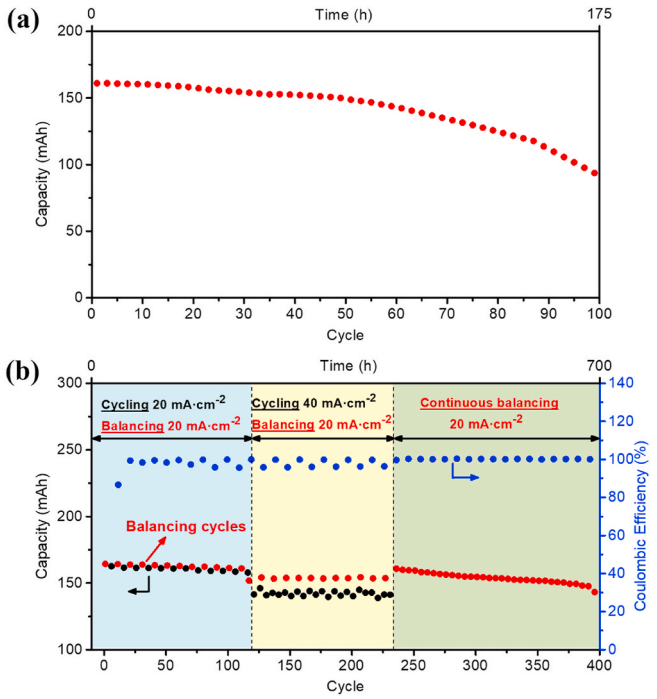

Fig. 5. Electrochemical performance of an anthraquinone//$K_4Fe(CN)_6$ system (20 mL of 0.3 M $K_4Fe(CN)_6$ and 10 mL of 0.3 M DHAQ) in 1.5 M KOH under N_2 atmosphere. **(a)** Charge capacity for over 100 cycles at 20 $mAcm^{-2}$ applying typical operation conditions. **(b)** Charge capacity applying the balancing protocol. During first section, the cell was cycled at 20 $mAcm^{-2}$ (cut-off at 1.6V) including a balancing cycle at 20 $mAcm^{-2}$ (cut-off at 2V) every 10 cycles. During second section, balancing cycles were maintained while the rest were increased to 40 $mAcm^{-2}$. Last cycles were carried out at 20 $mAcm^{-2}$ with a cut-off of 2 V.

side reactions, e.g. ORR and HER. They showed that the state of charge strongly influences this dimerization process and, as a consequence, the capacity decay: the higher the state of charge, the faster capacity decay. Indeed, the reported value of capacity fading increased up to 0.23% h^{-1} when cycled at 99.9% state of charge [25]. It is worth highlighting that this value reported in the literature is identical to the value obtained in this work when no balancing protocol is applied. Considering that our batteries were cycled at 100% depth of charge, the good capacity decay value of 0.0099% h^{-1} obtained by employing the balancing protocol suggests that faradaic imbalance likely contributed to the poor value of 0.24% h^{-1} previously reported [25] when cycled at 100% depth of charge. In our measurements, the osmotic imbalance between the two electrolytes provoked a slow water transport from the positive to the negative compartment, which eventually led to the end of the experiment (700 h). It should be noted that consumption of water for the OER does not contribute significantly to this imbalance of volumes. 1 mL of water provides almost 3.000 mAh through the OER. Under N_2-atmosphere, 1 mL of water can balance our system for 3.000 cycles since charge imbalance accounts for <1 mAh per cycle under N_2-atmosphere,.

Alkaline ferrocyanide electrolyte has been demonstrated to efficiently operate when paired with various organic compounds, as for the case of phenazine derivatives [26]. The proposed electrochemical balancing protocol was then extended to this system to elucidate whether the approach is also beneficial for other battery chemistries. Fig. 6a shows the relatively fast capacity decay of a DHPS//$K_4Fe(CN)_6$ flow battery operated at 40 mA cm^{-2} under an N_2 atmosphere. It should be noted that charge capacity remained stable for the first ~15 cycles, which could be explained by a slight excess of the capacity of $K_4Fe(CN)_6$ solution compared to the DHPS one: capacities of 160 mAh and 150 mAh were reached in the first discharge cycle for AQ//$K_4Fe(CN)_6$ and

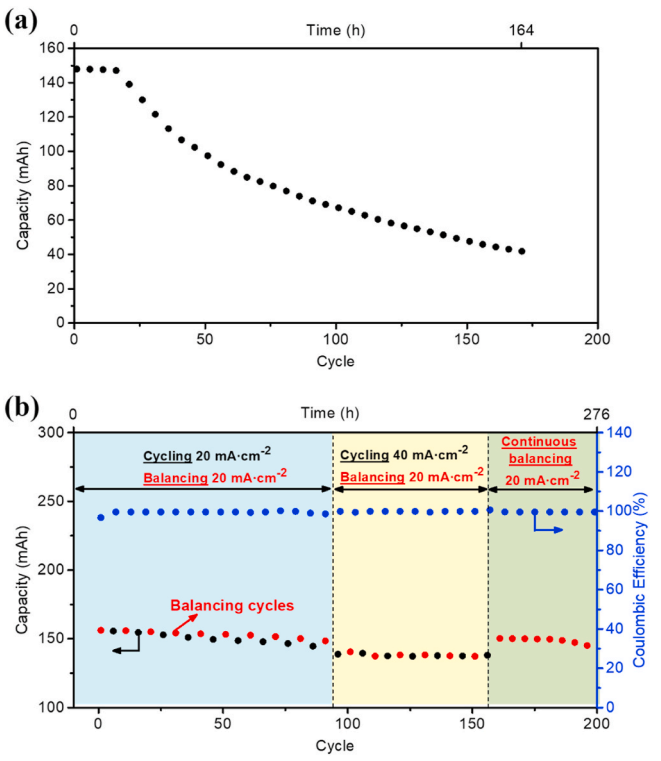

Fig. 6. Electrochemical performance of a phenazine derivative//$K_4Fe(CN)_6$ system (20 mL of 0.3 M $K_4Fe(CN)_6$ and 10 mL of 0.3 M DHPS) in 1 M KOH under N_2 atmosphere. (a) Charge capacity for over 100 cycles at 20 $mAcm^{-2}$ applying typical operation conditions. (b) Charge capacity applying the balancing protocol. During the first section, the cell was cycled at 20 $mAcm^{-2}$ (cut-off at 1.7 V) including a balancing cycle at 20 $mAcm^{-2}$ (cut-off at 2 V) every 10 cycles. During the second section, balancing cycles were maintained while the rest were increased to 40 $mAcm^{-2}$. Last cycles were carried out at 20 $mAcm^{-2}$ with a cut-off of 2.0 V.

DHPS//$K_4Fe(CN)_6$, respectively, using the same amount (moles) of ferrocyanide so that 10 mAh of ferrocyanide remined "unused" for DHPS//$K_4Fe(CN)_6$, in the first cycle. Once the excess was consumed, a pronounced capacity fading was observed for 175 cycles resulting in decay values of 0.44%·h^{-1} and 0.41%·$cycle^{-1}$. The implementation of the electrochemical balancing protocol resulted in a remarkable improvement of the cycle stability, retaining 94% of its initial storage capacity after 190 cycles (267 h) and reducing the capacity decay down to 0.017%·h^{-1} (0.023%·$cycle^{-1}$) for a comparable 175 cycle-period (Fig. 6b). This value is lower than the 0.039% h^{-1} reported using a similar concentration of species (0.1 M phenazine) and an Ar-filled glovebox (complete absence of O_2) [26]. It should be noted that the osmotic imbalance between the electrolytes was more severe in the case of DHPS//$K_4Fe(CN)_6$, which prevents us to evaluate a larger number of cycles. Thus, once the faradaic imbalance is mitigated by the implementation of the electrochemical balancing strategy, the osmotic imbalance between the two electrolytes appears to become a major issue when evaluating long-term cycle stability for the two studied cases.

Although this strategy is originally conceived as a tool for battery research at lab-scale enabling the deconvolution of the faradaic imbalance from other sources of capacity fading in AORFBs (degradation, cross-over, etc), it can potentially be of interest for larger-scale application. In that case, preventing corrosion of the graphite felts will be the main challenge, which may be addressed by adding small amounts of the OER catalyst, e.g. $Ni(OH)_2$ nanoparticles in the positive reservoirs that stick onto the electrode surface by stable electrostatic forces [27], to promote the OER in the catalytic material. The energy cost of this approach is related to the oxygen diffusion rate into the system. In our case, the coulombic efficiency stabilized at 99.5%. It means that our approach should correct 0.5% per cycle. Since the cell voltage of the balancing process is 50% higher than the nominal cell voltage, the energy required for the balancing step is about 0.75% of the energy stored in the system. In other words, the electrochemical balancing protocol decreases the round-trip efficiency of the system by 0.75%.

3. Conclusion

AORFBs face several challenges for achieving relevant long-term cycle stabilities, i.e. degradation of the active materials, cross-over of active species through the membrane, or faradaic imbalance. While the two former issues have long been recognized and attempted to be addressed, the latter issue attracted little attention. In this work, we showed that faradaic imbalance is not a negligible issue, seriously compromising the cycle stability of well-performing battery chemistries. The existence of irreversible side reactions is responsible for the faradaic imbalance, leading to an uneven state of charge of the anolyte and catholyte.

A strategy to prevent and/or reverse the capacity fading due to the occurrence of side reactions is demonstrated herein. This approach is based on lifting the uppercut-off voltage during the charging process to intentionally promote either the HER or the OER to balance the state of charge of both electrolytes. The approach has been demonstrated for balancing an AORB, previously imbalanced by exposing the anolyte to air. The promoted oxygen-related reduction reaction (the electrochemical ORR and oxidation of reduced species by oxygen present in the negative electrolyte) occurring at the negative electrode during charging led to a rapid capacity decay. The implementation of an electrochemical balancing cycle (one charging process using a higher value for the upper cutoff voltage) reestablished the initial capacity, leading up to a 50% increase in the charge capacity in just one cycle. This strategy was extended to other battery chemistries, indicating that it could be a general approach for any AORFB. In the two case studies, the implementation of this simple charging procedure led to a remarkable 20-fold reduction of capacity fading(% h^{-1}). This simple methodology is expected to contribute to the enhancement of the cycling stability, ruling out one of the major contributors to the capacity fading or avoiding the use of expensive equipment, e.g. O_2-excluding glovebox.

4. Experimental section

4.1. Materials

All chemicals were purchased from Sigma Aldrich and used as received.

Synthesis of 7,8-dihydroxyphenazine-2-sulfonic acid (DHPS).

7,8-dihydroxyphenazine-2-sulfonic acid was prepared by following the described procedure previously reported [26].

4.2. Preparation of electrolytes

In the DHPS//$K_4Fe(CN)_6$ flow cell, the catholyte was prepared by dissolving potassium ferrocyanide (2.5 g) in 1 M KOH to afford 20 mL 0.3 M ferrocyanide. The anolyte was prepared by dissolving 0.87 g of 7,8-dihydroxyphenazine-2-sulfonic acid in 1.9 M KOH to afford 10 mL 0.3 M phenazine (0.6 M eq. considering the exchange of 2 electrons) and 1 M KOH.

In the DHAQ//$K_4Fe(CN)_6$ flow cell, the catholyte was prepared by dissolving potassium ferrocyanide (2.5 g) in 1.5 M KOH to afford 20 mL 0.3 M ferrocyanide. The anolyte was prepared by dissolving 2,6-dihydroxyanthraquinone (1.27 g) in 2.1 M KOH to afford 10 mL 0.3 M 2,6-DHAQ and 1.5 M KOH.

Deionized water was used to prepare the electrolytes, and 2,6-DHAQ and DHPS electrolytes were purged with nitrogen prior to use.

4.3. Flow batteries

Filter-pressed flow cells using Nafion 212 and graphite felt as the ion selective membrane and electrodes were used in this study. The projected area of the cell was 9 cm^2. The flow rate was fixed at ca. 50 mL min^{-1}.

Electrochemical characterization. Galvanostatic charge-discharge measurements were conducted using a Biologic VMP multichannel potentiostat. The batteries were galvanostatically charged at 40 mA cm^{-2} and 20 $mAcm^{-2}$ with voltage limits of 1.6 V for anthraquinone, 1.7 V for phenazine. Subsequently, it was discharged at current densities between −40 and −20 $mAcm^{-2}$ with a voltage limit of 0.8 V under N_2 atmosphere, if otherwise is not specified.

Declaration of competing interest

The authors declare that they have no known competing financial interests or personal relationships that could have appeared to influence the work reported in this paper.

Acknowledgements

MFreeB project has received funding from the European Research Council (ERC) under the European Union's Horizon 2020 research and innovation programme (grant agreement No. 726217). The results reflect only the authors' view and the Agency is not responsible for any use that may be made of the information they contain. The authors also acknowledge the financial support by the Spanish Government through the Research Challenges Programme (Grant RTI2018-099228-A-I00). E. V. thanks the MINECO for the financial support (RYC2018-026086-I). A. M.-C. thanks the MINECO for the financial support (RYC2017-22700).

Appendix A. Supplementary data

Supplementary data to this article can be found online at https://doi.org/10.1016/j.jpowsour.2021.230516.

Author statement

Teresa Paez: Methodology, Investigation, Visualization, Writing-Original draft. **Alberto Martinez- Cuezva**: Investigation, Resources. **Rebeca Marcilla**: Supervision, Funding acquisition **Jesús Palma**: Supervision, Funding acquisition. **Edgar Ventosa**: Conceptualization, Methodology, Writing - Review & Editing, Supervision, Funding acquisition.

References

[1] B. Dunn, H. Kamath, J.M. Tarascon, Electrical energy storage for the grid: a battery of choices, Science 334 (2011) 928–935, https://doi.org/10.1126/science.1212741.
[2] Z. Yang, J. Zhang, M.C.W. Kintner-Meyer, X. Lu, D. Choi, J.P. Lemmon, J. Liu, Electrochemical energy storage for green grid, Chem. Rev. 111 (2011) 3577–3613, https://doi.org/10.1021/cr100290v.
[3] M.L. Perry, A.Z. Weber, Advanced redox-flow batteries: a perspective, J. Electrochem. Soc. 163 (2016), https://doi.org/10.1149/2.0101601jes. A5064–A5067.
[4] G.L. Soloveichik, Battery technologies for large-scale stationary energy storage, Annu. Rev. Chem. Biomol. Eng. 2 (2011) 503–527, https://doi.org/10.1146/annurev-chembioeng-061010-114116.
[5] C. Ding, H. Zhang, X. Li, T. Liu, F. Xing, Vanadium flow battery for energy storage: prospects and challenges, J. Phys. Chem. Lett. 4 (2013) 1281–1294, https://doi.org/10.1021/jz4001032.
[6] M. Ulaganathan, V. Aravindan, Q. Yan, S. Madhavi, M. Skyllas-Kazacos, T.M. Lim, Recent advancements in all-vanadium redox flow batteries, Adv. Mater. Interfaces 3 (2016) 1–22, https://doi.org/10.1002/admi.201500309.
[7] J. Winsberg, T. Hagemann, T. Janoschka, M.D. Hager, U.S. Schubert, Redox-flow batteries: from metals to organic redox-active materials, Angew. Chem. Int. Ed. (2016) 2–28, https://doi.org/10.1002/anie.201604925.
[8] E. Sánchez-Díez, E. Ventosa, M. Guarnieri, A. Trovò, C. Flox, R. Marcilla, F. Soavi, P. Mazur, E. Aranzabe, R. Ferret, Redox flow batteries: status and perspective towards sustainable stationary energy storage, J. Power Sources 481 (2021) 228804, https://doi.org/10.1016/j.jpowsour.2020.228804.
[9] K. Wedege, E. Dražević, D. Konya, A. Bentien, Organic redox species in aqueous flow batteries: redox potentials, chemical stability and solubility, Sci. Rep. 6 (2016) 1–13, https://doi.org/10.1038/srep39101.
[10] Q. Chen, L. Eisenach, M.J. Aziz, Cycling analysis of a quinone-bromide redox flow battery, J. Electrochem. Soc. 163 (2016), https://doi.org/10.1149/2.0081601jes. A5057–A5063.
[11] M. Skyllas-Kazacos, Thermal stability of concentrated V(V) electrolytes in the vanadium redox cell, J. Electrochem. Soc. 143 (1996) L86, https://doi.org/10.1149/1.1836609.
[12] Z. Wei, A. Bhattarai, C. Zou, S. Meng, T.M. Lim, M. Skyllas-Kazacos, Real-time monitoring of capacity loss for vanadium redox flow battery, J. Power Sources 390 (2018) 261–269, https://doi.org/10.1016/j.jpowsour.2018.04.063.
[13] C. Sun, J. Chen, H. Zhang, X. Han, Q. Luo, Investigations on transfer of water and vanadium ions across Nafion membrane in an operating vanadium redox flow battery, J. Power Sources 195 (2010) 890–897, https://doi.org/10.1016/j.jpowsour.2009.08.041.
[14] A.A. Shah, H. Al-Fetlawi, F.C. Walsh, Dynamic modelling of hydrogen evolution effects in the all-vanadium redox flow battery, Electrochim. Acta 55 (2010) 1125–1139, https://doi.org/10.1016/j.electacta.2009.10.022.
[15] H. Al-Fetlawi, A.A. Shah, F.C. Walsh, Modelling the effects of oxygen evolution in the all-vanadium redox flow battery, Electrochim. Acta 55 (2010) 3192–3205, https://doi.org/10.1016/j.electacta.2009.12.085.
[16] A. Tang, J. Bao, M. Skyllas-Kazacos, Dynamic modelling of the effects of ion diffusion and side reactions on the capacity loss for vanadium redox flow battery, J. Power Sources 196 (2011) 10737–10747, https://doi.org/10.1016/j.jpowsour.2011.09.003.
[17] E.W. Zhao, T. Liu, E. Jónsson, J. Lee, I. Temprano, R.B. Jethwa, A. Wang, H. Smith, J. Carretero-González, Q. Song, C.P. Grey, In situ NMR metrology reveals reaction mechanisms in redox flow batteries, Nature 579 (2020) 224–228, https://doi.org/10.1038/s41586-020-2081-7.
[18] Y. Ji, M. Goulet, D.A. Pollack, D.G. Kwabi, S. Jin, D. Porcellinis, E.F. Kerr, R. G. Gordon, M.J. Aziz, A phosphonate-functionalized quinone redox flow battery at near-neutral pH with record capacity retention rate, Adv. Energy Mater. 9 (2019) 1900039, https://doi.org/10.1002/aenm.201900039.
[19] R.A. Potash, J.R. McKone, S. Conte, H.D. Abruña, On the benefits of a symmetric redox flow battery, J. Electrochem. Soc. 163 (2016), https://doi.org/10.1149/2.0971602jes. A338–A344.
[20] T. Jirabovornwisut, A. Arpornwichanop, A review on the electrolyte imbalance in vanadium redox flow batteries, Int. J. Hydrogen Energy 44 (2019) 24485–24509, https://doi.org/10.1016/J.IJHYDENE.2019.07.106.
[21] O. Nolte, I.A. Volodin, C. Stolze, M.D. Hager, U.S. Schubert, Trust is good, control is better: a review on monitoring and characterization techniques for flow battery electrolytes, Mater. Horizons. 8 (2021) 1866–1925, https://doi.org/10.1039/D0MH01632B.
[22] Z. Li, L. Liu, Y. Zhao, J. Xi, Z. Wu, X. Qiu, The indefinite cycle life via a method of mixing and online electrolysis for vanadium redox flow batteries, J. Power Sources 438 (2019) 226990, https://doi.org/10.1016/J.JPOWSOUR.2019.226990.
[23] N. Poli, M. Schäffer, A. Trovò, J. Noack, M. Guarnieri, P. Fischer, Novel electrolyte rebalancing method for vanadium redox flow batteries, Chem. Eng. J. 405 (2021) 126583, https://doi.org/10.1016/J.CEJ.2020.126583.
[24] E.S. Beh, D. De Porcellinis, R.L. Gracia, K.T. Xia, R.G. Gordon, M.J. Aziz, A neutral pH aqueous organic- organometallic redox flow battery with extremely high capacity retention, ACS Energy Lett 2 (2017) 639–644, https://doi.org/10.1021/acsenergylett.7b00019.
[25] M.A. Goulet, L. Tong, D.A. Pollack, D.P. Tabor, S.A. Odom, A. Aspuru-Guzik, E.E. Kwan, R.G. Gordon, M.J. Aziz, Extending the lifetime of organic flow batteries via redox state management, J. Am. Chem. Soc. 141 (2020) 8014-8019. https://doi.org/10.1021/jacs.8b13295.
[26] A. Hollas, X. Wei, V. Murugesan, Z. Nie, B. Li, D. Reed, J. Liu, V. Sprenkle, W. Wang, A biomimetic high-capacity phenazine-based anolyte for aqueous organic redox flow batteries, Nat. Energy. 3 (2018) 508–514, https://doi.org/10.1038/s41560-018-0167-3.
[27] S. Barwe, J. Masa, C. Andronescu, B. Mei, W. Schuhmann, E. Ventosa, Overcoming the instability of nanoparticle-based catalyst films in alkaline electrolyzers by using self-assembling and self-healing films, Angew. Chem. Int. Ed. 56 (2017) 8573–8577, https://doi.org/10.1002/ANIE.201703963.